Electronic Supplementary Information

Surfactant-assisted ammonium vanadium oxide as superior cathode for calcium ion batteries

Thuan Ngoc Vo [a], Hyeongwoo Kim[b,c], Jaehyun Hur [a], Wonchang Choi[b,d**††], Il Tae Kim[a,*†]

[a] Department of Chemical and Biological Engineering, Gachon University, 13120, Republic of Korea.

[b] Centre for Energy Storage Research, Korea Institute of Science and Technology, 5, Hwarang-ro 14-gil, Seongbuk-gu, Seoul 02792, Republic of Korea

[c] Department of Materials Science and Engineering, Korea University, 145, Anam-ro, Seongbuk-gu, Seoul 02841, Republic of Korea

[d] Division of Energy & Environment Technology, KIST School, Korea University of Science and Technology, 5, Hwarang-ro 14-gil, Seongbuk-gu, Seoul 02792, Republic of Korea

† Phone: +82-31-750-8835, Fax: +82-31-750-5363, Email: itkim@gachon.ac.kr

††Phone: +82-2-958-5253, Fax: +82-958-5229, Email: wonchangchoi@kist.re.kr

Table S1. Results from ELS of NVO and NVO@SBDS samples.

	Mean diameter (nm)	Standard Deviation (nm)	Polydisperisity index
NVO	575.2	257.9	0.201
NVO@SDBS	401.1	18.4	0.002

*The Polydisperisity index (PDI) was calculated as[1]:

$$PDI = \left(\frac{\sigma}{2a}\right)^2$$

Where σ : standard deviation of sample

2a : mean diameter

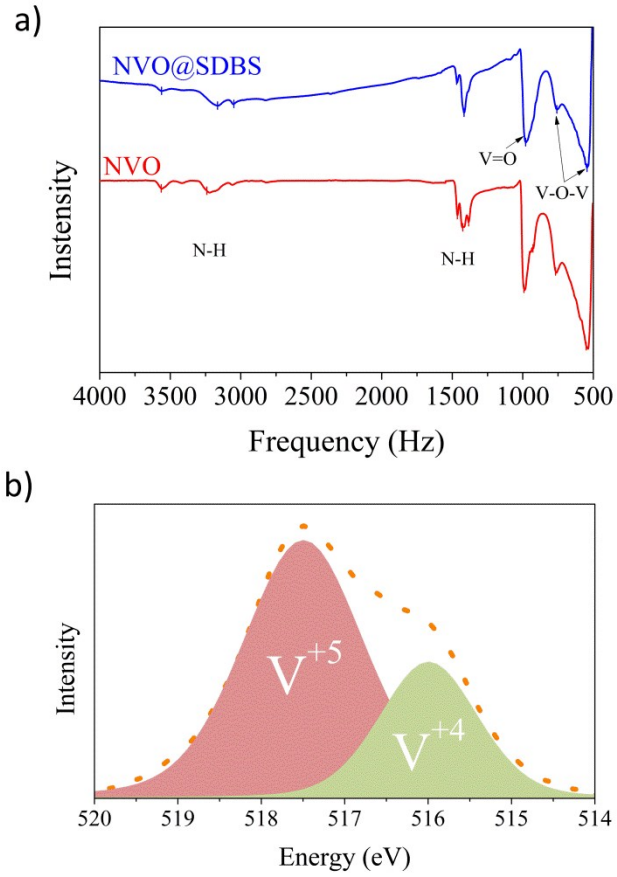

Figure S1. (a) FTIR of NVO and NVO@SDBS; (b) High-resolution XPS spectra with peak integration of V 2p for NVO@SDBS.

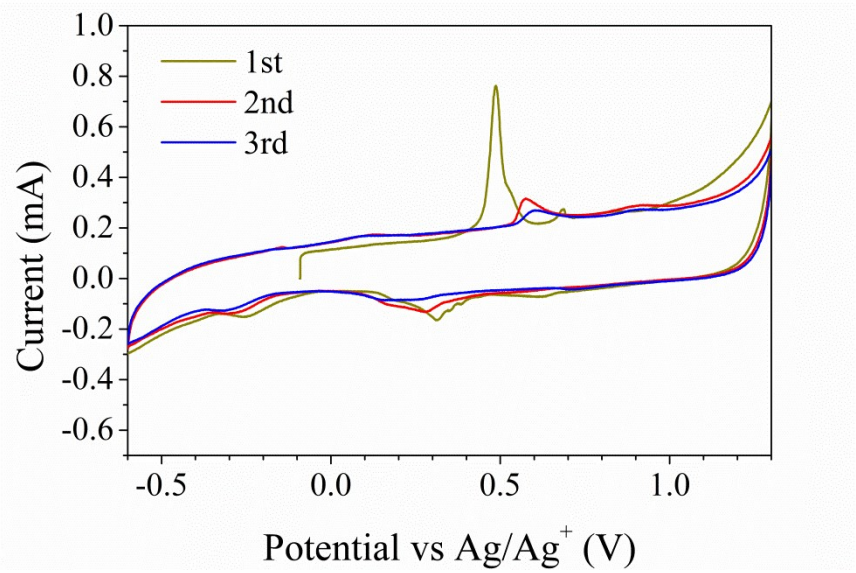

Figure S2. Cyclic voltammograms of NVO with electrolyte of 1M $Ca(ClO_4)_2$ in acetonitrile from - 0.6 V to 1.3 V vs. silver ion reference at a scan rate of 0.5 mV s^{-1}.

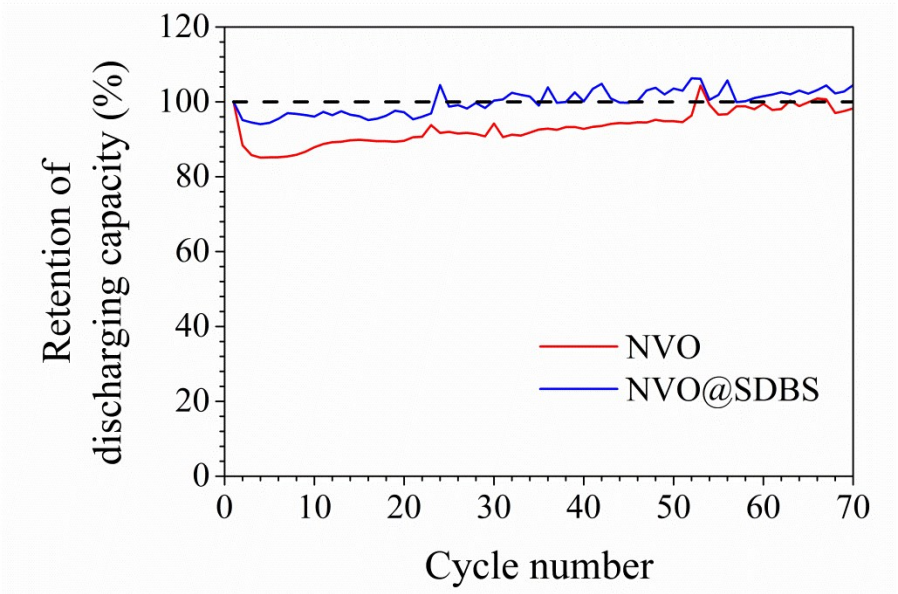

Figure S3. Discharge capacity retentions of NVO and NVO@SDBS electrodes.

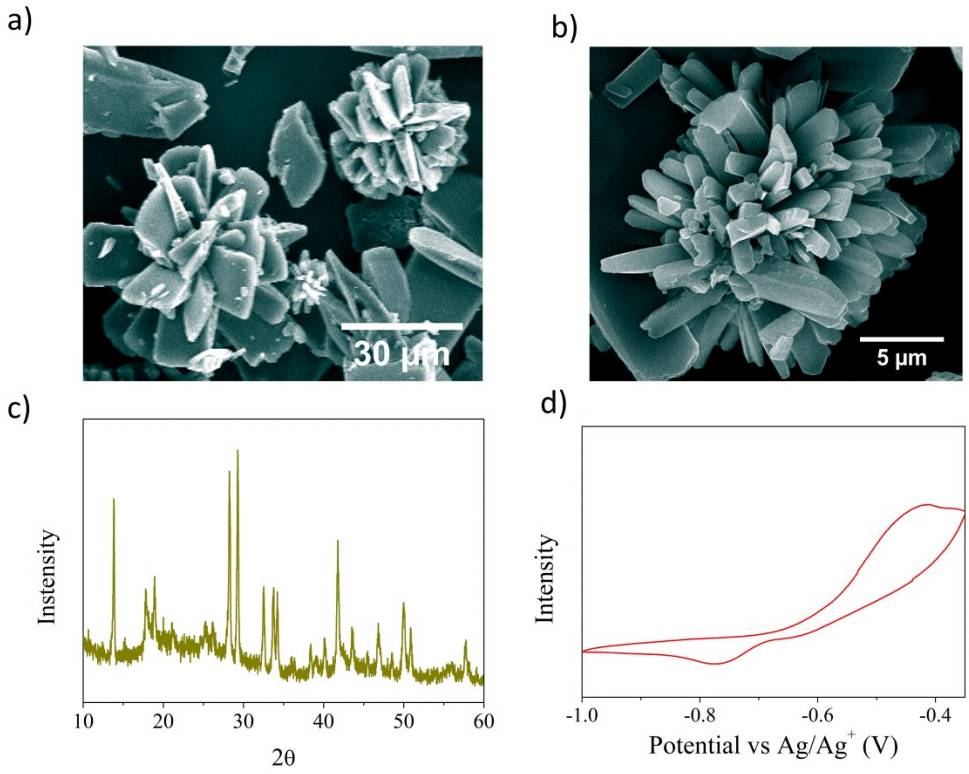

Figure S4. (a, b) SEM images, (c) XRD pattern, and (d) Cyclic voltammogram of the as-prepared Mn-bdcNH$_2$.

Figure S4(a) and (b) show the as-prepared Mn-bdcNH$_2$ anode material. It has a micro-flower shape consisting of flat plates. From the XRD pattern, the obtained Mn-bdcNH$_2$ material has a high crystallinity as seen in Fig. S4(c). Cyclic voltammogram in Fig. S4(d) shows a cathodic peak at -0.77 V and an anodic peak at -0.43 V vs. Ag/Ag$^+$ representing the possible insertion/desertion of Ca ions into/from anode.

Simulation method for V_4O_{10} and $Ca_{0.5}V_4O_{10}$ structures:

All of the simulation was based on the minimization of system's total energy with Quantum Espresso Software v.5.3.0. We used ultra-soft pseudopotential packages for all atoms with PBE-type exchange-correlation functional. The unit cell was firstly variable-cell relaxed (vc-relax mode) to define fractional coordination of atoms in the unit cell with initial guess of K-mesh as 4 x 4 x 4 and kinetic energy cut off for wave function (ecutwfc) as 40.0 Rydberg (Ry). Because of the ultra-soft pseudopotential, kinetic energy cut off for charge density and potential (ecutrho) was eight times of ecutwfc. In addition, David diagonalization with plain-type mixing mode was applied. The convergence threshold was 10^{-6} for the whole optimization. The desired internal stress of the unit cells was defined as 0.02 k-bar in vc-relax mode.

After relaxation step, the goodness of the initial ecutwfc and K-mesh were rechecked by drawing the relations of those parameters to the total energy of the unit cell. We optimized the unit cell volume without changing relaxed 'b/a', 'c/a' and 'γ'. Total forces and stresses were also calculated to confirm the fineness of the optimization. Simulated results were presented in Table S2.

For the simulation of V_4O_{10}, the unit cells were obtained by minimizing the total energy and rechecking total force and stress as shown in Fig. S5. When varying the ecutwfc from 10 Ry to 45 Ry, the total energies were continuously decreased from -1675.13 Ry and then converged to -1808.38 Ry at an ecutwfc of 40 Ry (Fig. S5(a)). Fig. S5(b) shows the total energies were converged to -1808.32 Ry at K-mesh as 3 x 3 x 3. Based on the optimized ecutwfc and K-mesh, Fig. S5(c) illustrates that the dependence of total energy on cell volume from 2576 a.u.^{3} to 2954 a.u.^{3} could be well fitted with a parabolic shape (the coefficient of determination is ~ 99.9%). The optimized volume (2839.76 a.u.^{3}) was taken at the minimum point of the fitted curve. The determined volume also matched with the smallest total force (Fig. S5(d)), which made the total stress of the cell to be ~ 0 kbar (Fig. S5(e)), proving the truthfulness of the relaxation. Similarly, Fig. S6 describes the optimization of the relaxation of $Ca_{0.5}V_4O_{10}$ structure. The optimization process generated the values of ecutwfc, K-mesh and cell volume as 35.0 Ry, 3 x 3 x 3 and 2770.61 a.u.^{3}, respectively.

Table S2. Cell parameters of simulated V_4O_{10} and $Ca_{0.5}V_4O_{10}$ structures.

	a (A)	b (A)	c (A)	(α,β,γ)	Unit cell volume (A^3)
V_4O_{10}	11.70	3.60	10.14	(90,100.16,90)	420.81
$Ca_{0.5}V_4O_{10}$	11.61	3.67	9.83	(90,100.89,90)	410.56

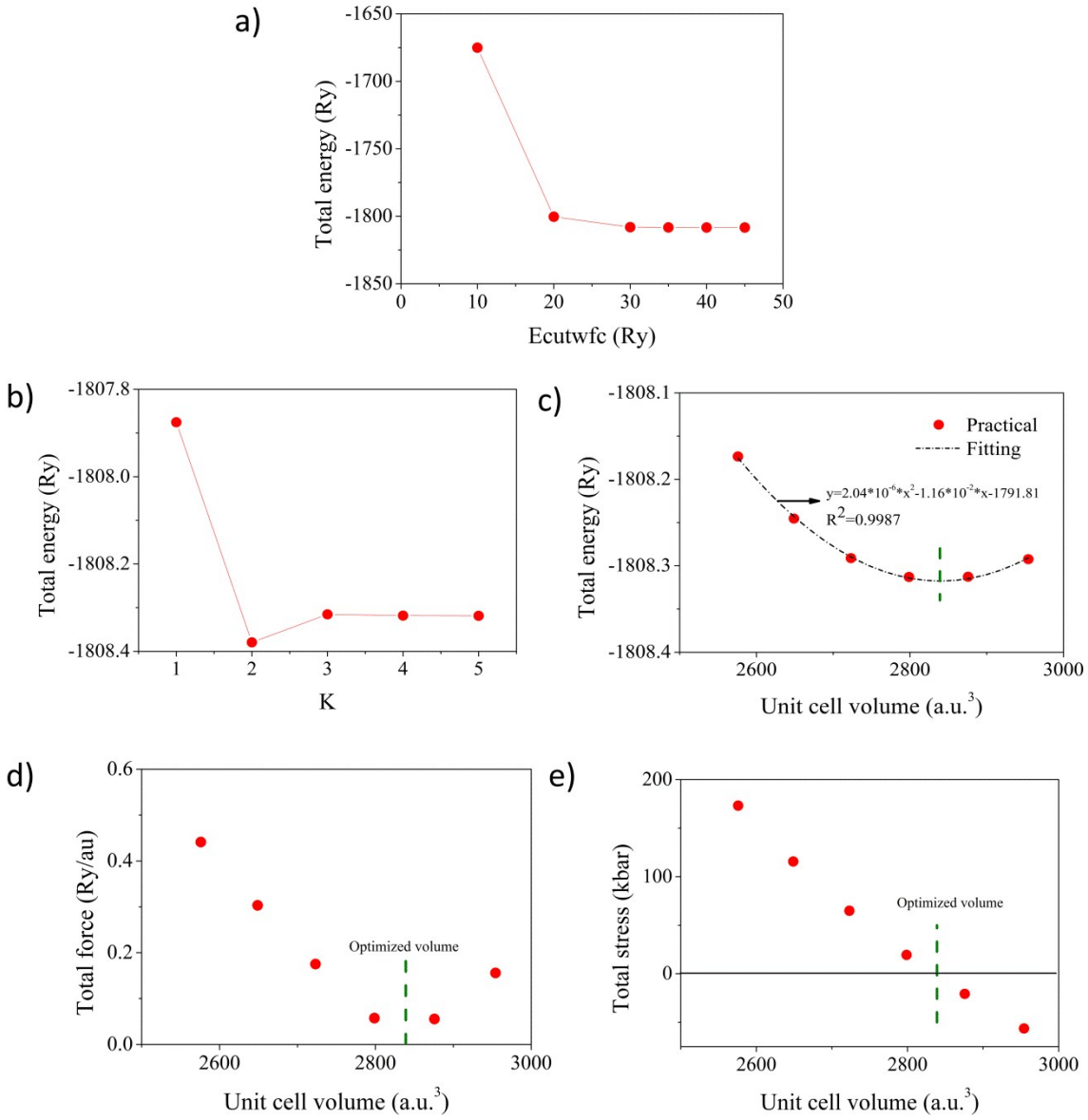

Figure S5. Simulation results of V_4O_{10} structure. Dependency of total energy on (a) kinetic cutoff energy, (b) K, and (c) unit cell volume. Variations of (d) total force and (e) internal stress to unit cell volume.

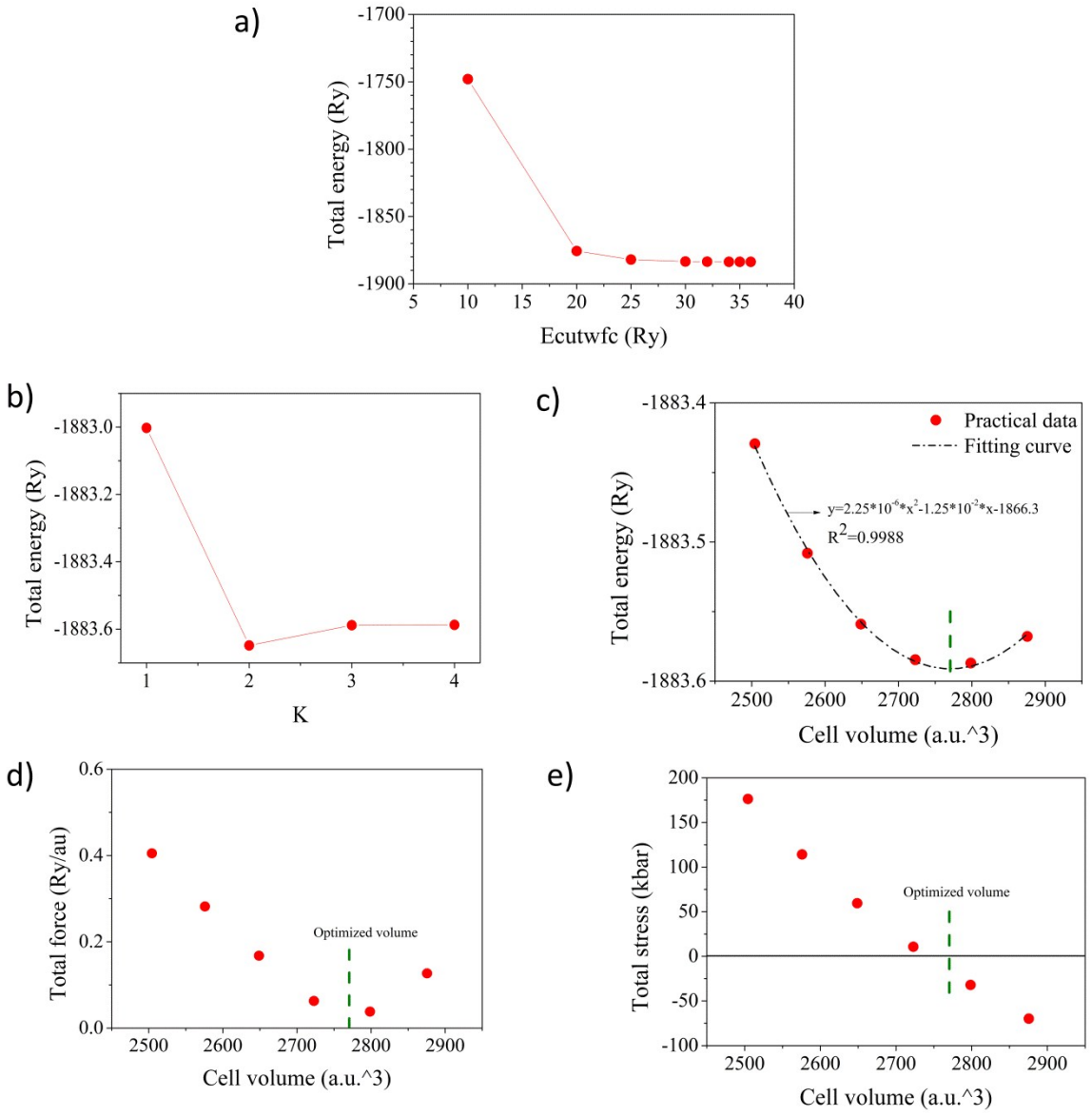

Figure S6. Simulation results of $Ca_{0.5}V_4O_{10}$ structure. Dependency of total energy on (a) the kinetic cutoff energy, (b) K, and (c) unit cell volume. Variations of (d) total force and (e) internal stress to unit cell volume.

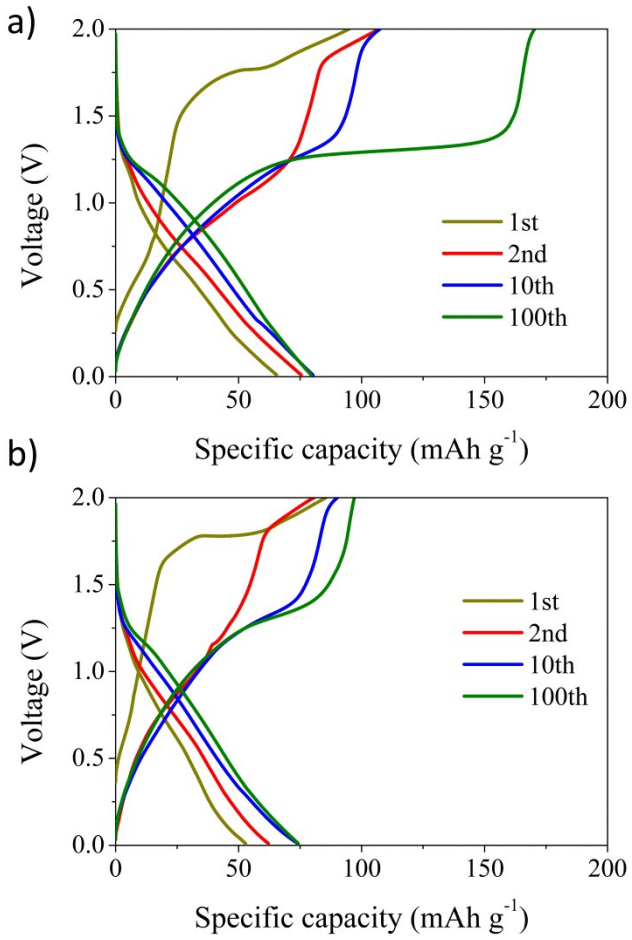

Figure S7. Galvanostatic charge-discharge profiles of full cell with Mn-bdcNH$_2$ anode and (a) NVO cathode, and (b) NVO@SDBS cathode from 0.01 V to 2 V at a current density of 0.1 A g^{-1}.

Figure S7 shows the voltage profiles of full cells with Mn-bdcNH$_2$ anode and NVO/ NVO@SDBS cathode. During the first charge, the cell with NVO showed two slopping plateaus at 1.7 V and 1.8 V representing the desertions of ammonium ions (Fig. S7(a)). However, due to the replacement of ammonium ion with Ca ion, the charge-discharge curves did not have clear plateaus from the second cycle, which also happened in full cell with NVO@SDBS (Fig. S7(b)). Interestingly, continuous cycling became to reveal a clear plateau at ~ 1.3 V during the charging step. The plateau at ~ 1.3 V could be related to the irreversible redox reactions happening during the charge steps, which causes the low efficiencies in the full cells. Indeed, the full cell with NVO revealed significant increase in the irreversible reactions at ~ 1.3 V compared to that of the cell with NVO@SDBS, leading to low coulombic efficiency. Therefore, it is believed that uniform and small size of NVO@SDBS electrode could help to reduce the unknown irreversible reactions when comparing to non-uniform and big size of NVO electrode.

Table S3. Comparison on the electrochemical performance of cathode materials for calcium-ion batteries.

	Ref.	Working electrode	Reference electrode	Counter electrode	Current density (mA g^{-1})	Maximum discharge capacity (mAh g^{-1}) from potential ranges (V) vs Ref. electrode	Capacity retention(%) after cycles	Average coulombic efficiency
Three electrode system	2	$K_2BaFe(CN)_6$	Ag/AgCl (sat. KCl)	Graphite	10	~ 56 from -0.25 V to 0.5 V	~ 100 % After 30 cycles	~ 94 %
	3	$KFeFe(CN)_6$	Ag/Ag^+ in CH_3CN	Graphite	125	~ 140 from -0.14 V to 1.3 V	~ 75 % After 80 cycles	-
	4	$CuFe(CN)_6$	Saturated calomel electrode (SCE)	Activated carbon	850	~ 70 from 0 V to 1 V	~ 88.6 % After 5000 cycles	~ 98.1 %
	Our work	monodisperse $NH_4V_4O_{10}$	Ag/Ag^+ in CH_3CN	Pt coil	100	~ 150 from -0.3 V to 1 V	~ 100 % After 100 cycles	90-95%
	Ref.	Cathode	Anode		Current density (mA g^{-1})	Maximum discharge capacity (mAh g^{-1})	Capacity retention(%) after cycles	Average coulombic efficiency
Two electrode system (Full cell)	5	$CaCo_2O_4$	V_2O_5		50	~ 100 from -1.25 V to 2.25 V	~ 75 % After 30 cycles	~ 40 %
	6	Na_2FePO_4F	Ca-metal pseudo reference		10	~ 80 from -1.5 V to 3 V	-	~ 84 %
	7	$KNiFe(CN)_6$	Activated carbon		250	~ 35 from 0.22 V to 0.92 V (vs SHE)	~ 53 % After 2000 cycles	~ 99.5 %
	8	$Na_xMnFe(CN)_6$	Calciated tin		10	~ 100 from 0 V to 4 V	~ 50 % After 35 cycles	~ 90%
	9	Graphite	Sn		100	~ 85 from 3 V to 5 V	~ 95 % After 350 cycles	~ 80 %
	10	Expanded graphite	Mesocarbon microbeads		66	~ 66 from 3 V to 5.2 V	~ 94 % After 300 cycles	~ 85 %
	Our work	monodisperse $NH_4V_4O_{10}$	Manganese 2-aminoterephthalate		100	~ 75 from 0.01 V to 2 V	~ 100 % After 100 cycles	~ 80%

Reference

1. H. J. M., B. P. M., G. Andrew, D. Pranab, T. Karen and L. John, *J. Appl. Polym. Sci.*, 2015, **132**.

2. P. Padigi, G. Goncher, D. Evans and R. Solanki, *J. Power Sources*, 2015, **273**, 460-464.

3. N. Kuperman, P. Padigi, G. Goncher, D. Evans, J. Thiebes and R. Solanki, *J. Power Sources*, 2017, **342**, 414-418.

4. C. Lee and S.-K. Jeong, *Electrochim. Acta*, 2018, **265**, 430-436.

5. M. Cabello, F. Nacimiento, J. R. González, G. Ortiz, R. Alcántara, P. Lavela, C. Pérez-Vicente and J. L. Tirado, *Electrochem. commun.*, 2016, **67**, 59-64.

6. A. L. Lipson, S. Kim, B. Pan, C. Liao, T. T. Fister and B. J. Ingram, *J. Power Sources*, 2017, **369**, 133-137.

7. R. Y. Wang, C. D. Wessells, R. A. Huggins and Y. Cui, *Nano Lett.*, 2013, **13**, 5748-5752.

8. A. L. Lipson, B. Pan, S. H. Lapidus, C. Liao, J. T. Vaughey and B. J. Ingram, *Chem. Mater.*, 2015, **27**, 8442-8447.

9. M. Wang, C. Jiang, S. Zhang, X. Song, Y. Tang and H.-M. Cheng, *Nat. Chem.*, 2018, **10**, 667-672.

10. S. Wu, F. Zhang and Y. Tang, *Adv. Sci.*, 2018, **5**, 1701082.